Thermal Analysis of Isothermal Crystallization Kinetics in Blends of Cocoa Butter with Milk Fat or Milk Fat Fractions

Serpil Metin[a] and Richard W. Hartel[b,*]

[a]M&M/Mars, Inc., Hackettstown, New Jersey 07840, and [b]University of Wisconsin-Madison, Madison, Wisconsin 53706

ABSTRACT: The kinetics of isothermal crystallization of binary mixtures of cocoa butter with milk fat and milk fat fractions were evaluated by applying the Avrami equation. Application of the Avrami equation to isothermal crystallization of the fats and the binary fat blends revealed different nucleation and growth mechanisms for the fats, based on the Avrami exponent. The suggested mechanism for cocoa butter crystallization was heterogeneous nucleation and spherulitic growth from sporadic nuclei. For milk fat, the mechanism was instantaneous heterogeneous nucleation followed by spherulitic growth. For milk fat fractions, the mechanism was high nucleation rate at the beginning of crystallization, which decreased with time, and platelike growth. Addition of milk fat fractions did not cause a significant change in the suggested nucleation and growth mechanism of cocoa butter.

JAOCS 75, 1617–1624 (1998).

KEY WORDS: Avrami equation, cocoa butter, crystallization kinetics, DSC, fats, fractionation, isothermal crystallization, milk fat, milk fat fractions.

The nature of the fat phase of chocolate determines the properties of the final chocolate product. Cocoa butter is a major component of the fat phase of chocolate. In fact, cocoa butter contributes 30 to 40% by weight to finished chocolate and is responsible for the texture, gloss, and mouthfeel of the chocolate products (1). Typically, a long induction period is observed prior to initiation of crystallization of cocoa butter (2), reflecting the difficulty in producing stable nuclei. Rates of nucleation, growth, and polymorphic transformations of cocoa butter are important for controlling processing and storage conditions (3).

Milk fat is another important component of chocolate, especially milk chocolate. Up to 30% milk fat (on a fat basis) is used in milk chocolate, and it is often added at lower levels (5%) to dark chocolate to control hardness. The limiting factors for use of milk fat are technical rather than legislative. Crystallization of milk fat is more complicated than for most other fats due to its molecular complexity, the formation of mixed crystals, and different polymorphic modifications (4). The range of melting point (m.p.) and plasticity of milk fat limits its use in chocolate products, as it decreases the rate of cocoa butter crystallization and causes softening of chocolate and confectionery products (3,5,6). Milk fat does not affect the polymorphism of cocoa butter. However, the m.p. of each polymorph is lower in blends due to the complex lipid structure of milk fat (3,5,7).

In order to further increase use of milk fat in chocolate products, fractionation of milk fat into a range of products with different physical and chemical characteristics has been employed (8). However, effective replacement of cocoa butter with milk fat fractions is also limited, since crystallization behavior and kinetics of cocoa butter crystallization are affected by the interactions between the fats (3,9). Although crystallization of cocoa butter with added milk fat and/or milk fat fractions has been studied extensively (10–16), very little quantitative data are available describing the crystallization behavior and kinetics of the fat blends (17,18).

Thermal analysis methods such as dynamic thermal analysis and differential scanning calorimetry (DSC) have been used to determine isothermal transformation kinetics in many types of materials including metals, polymers, and glass-forming solids (19–26). The common features of these analyses are the use of the Avrami equation and an Arrhenius form for the temperature dependence of the reaction rate constant (24–27). So far, only a few studies have been reported for the application of isothermal Avrami kinetics to fats (28–31). The brief theory of the Avrami isothermal phase transformation kinetics will be given in the following section.

The objective of our study was to evaluate isothermal crystallization kinetics of binary fat blends of cocoa butter with milk fat and milk fat fractions by applying the Avrami equation.

The theory of Avrami isothermal phase transformation kinetics. The most general approach for description of isothermal phase transformation kinetics is the Avrami equation originally developed for polymers. In the 1940s, various authors independently developed this kinetic formulation, which is sometimes called the Johnson-Mehl-Avrami-Komogorov or Avrami kinetics equation (25,26). Isothermal Avrami kinetics is concerned with the overall crystallization

*To whom correspondence should be addressed at University of Wisconsin-Madison, 1605 Linden Dr., Madison, WI 53706.
E-mail: hartel@calshp.cals.wisc.edu

process, including nucleation and growth (26,32). The Avrami equation is given as (32)

$$(1–X) = \exp(–k\,t^n) \quad [1]$$

where X is fraction of crystal transformed at time t during crystallization, k is crystallization rate constant which depends primarily on crystallization temperature, and n, the Avrami exponent, is a constant relating to the dimensionality of the transformation. A comprehensive review of the derivation and development of the Avrami equation can be found in the works of Woldt (25) and Christian (27).

The Avrami exponent (n) is a function of the number of dimensions in which growth takes place, and reflects the details of nucleation and growth mechanisms (26). For most transformations, the n is found to be constant over a substantial range of temperature (26). The Avrami equation has been reported not only valid for linear growth (i.e., constant growth rate) but also for the early stages of diffusion-controlled growth (27). Christian (27) has tabulated some values of n expected for various transformation conditions. For example, an n of 4 indicates heterogeneous nucleation and spherulitic growth from sporadic nuclei, whereas an n of 3 also indicates spherulitic growth but from instantaneous nuclei. An n of 2 represents high nucleation rate and plate-like growth, where growth is primarily along two dimensions (27,32,33).

The crystallization rate constant, k, is a combination of nucleation and growth rate constants, and is a strong function of temperature (26). The temperature dependency of k is usually expressed by the Arrhenius equation (26). The numerical value of k is directly related to the half-time of crystallization, $t_{1/2}$, and therefore the overall rate of crystallization (34), which is given by the following equation:

$$(t_{1/2})^n = 0.693/k \quad [2]$$

Since thermal analysis techniques provide systems in which the time–temperature evaluation of the crystallization kinetics can be examined, they have been employed to study isothermal Avrami transformation kinetics (23–29). The heat released or absorbed during the transformation is monitored by DSC, the most common analytical technique used for application of the Avrami equation. The use of isothermal crystallization exotherms obtained by DSC to calculate the crystal fraction at a particular time will be discussed in a later section.

MATERIALS AND METHODS

Ivory Coast cocoa butter (ICCB) was supplied by Guittard Chocolate Company (Burlingame, CA). Anhydrous milk fat (AMF) from the winter feeding season was supplied by Level Valley Dairy (West Bend, WI). Milk fat fractions (six solid and one liquid) were obtained from the AMF by dry fractionation, as explained in a previous work (17). Milk fat fractions were designated according to the fractionation temperature and whether it is solid (S) or liquid (L) fraction. Additionally, milk fat fractions were classified into three classes according to the melting temperature (m.p.). These were very high-melting (m.p. > 45°C), high-melting (35°C < m.p. < 45°C), and low-melting (10°C < m.p. < 25°C) milk fat fractions. The fats used in this study are tabulated in Table 1 according to this general designation. Table 1 also includes solid fat content of the fats at 5 and 25°C, determined by nuclear magnetic resonance to give a better understanding of the melting profile. The fatty acid and triacylglycerol compositions of the component fats were reported previously (17). AMF and its fractions were incorporated into ICCB at 5 and 10% levels.

The m.p. The capillary m.p. (clear point) of ICCB, AMF, and AMF fractions were determined using AOCS method Cc-125 (35). Capillary m.p. of the component fats are given in Table 1.

Isothermal calorimetry. Isothermal analyses were performed by an automatic cooling DSC (DSC/5200, Seiko Instruments, Inc., Horsham, PA), attached to a disk station (SSC5200H). The DSC was calibrated with gallium, indium, and tin standards prior to analyses. Dry nitrogen gas was used to purge the thermal analysis system and liquid nitrogen was used to cool the system. Fat (5–12 mg) was sealed into an aluminum sample holder (TA Instruments, New Castle, DE). Changes in heat flow during isothermal DSC operation at crystallization temperature were recorded.

The following temperature protocol was used: hold at 80°C for 5 min, cool to 50°C at a rate of 100°C/min, hold for 3 min, cool at 100°C/min to crystallization temperature and hold for 3 h. Following 3 h isothermal hold, samples were

TABLE 1
General Designation of Component Fats

Fat type	Remarks
ICCB (M[a]-84[b],61[c],32[d])	Ivory Coast cocoa butter
AMF (H- 51,18,37)	Anhydrous milk fat from winter feeding season
SS (VH-73,58,49)	Super stearin (solid fraction of AMF-2 crystallized first at 27°C, then at 32°C)
32S (VH-69,53,48)	Solid fraction of AMF crystallized at 32°C
30S (VH-67,48,46)	Solid fraction of AMF crystallized at 30°C
28S (H-61,38,44)	Solid fraction of AMF crystallized at 28°C
23S (H-71,43,41)	Solid fraction of AMF crystallized at 23°C from the pooled fractions of 32, 30, and 28°C solid fractions
17S (L-59,9,23)	Solid fraction of AMF crystallized at 17°C from the liquid fraction of 23°C solid fraction
17L (L-23,0,12)	Liquid fraction of 17°C crystallization from the liquid fraction of 23°C solid fraction of AMF

[a]General melting property (VH = very high-melting, H = high-melting, M = medium-melting, L = low-melting).
[b]Solid fat content (SFC) at 5°C.
[c]SFC at 25°C.
[d]Capillary melting point.

heated to 80°C at a rate of 20°C/min to record melting profiles. Crystallization temperatures of 15, 20, and 25°C were studied, although the Avrami analysis was only performed on data obtained at 15°C.

Isothermal DSC data were used to evaluate kinetic parameters such as n, k, and $t_{1/2}$ by employing Equation 1. Equation 1 can be linearized by logarithmic transformation of $[-\ln (1 - X)]$ and t to calculate k and n from the intercept and slope, respectively.

Crystal fractions, or the relative amount of material crystallized, as a function of time were calculated by integration of the isothermal DSC crystallization curves (28) as shown in Figure 1. Integration of the crystallization curves at the determined time periods (starting from 5 min after zero time to the ending time of crystallization by 5-min intervals) was performed by image analysis. Each crystallization curve was digitized manually on a digitizer board (Model MM-1812; Sumagraphics, Fairchild, CT) connected to a computer (International Business Machines, Boca Raton, FL) equipped with image analysis software (Sigma Scan; Jandel Scientific, Sausalito, CA). The area under the exothermal crystallization curve corresponds to the total enthalpy of crystallization, ΔH_T. The crystal fraction (X) at a given time was approximated by the ratio of the partial enthalpy, ΔH_X, at that time to the total crystallization enthalpy. Average X value was taken from three replicates for each sample.

The $t_{1/2}$ was calculated by employment of the isothermal crystallization data to Equation 2.

Crystal structure. The crystal structure of component fats and binary fat blends were determined by X-ray diffractometer (XRD) at 17 ± 1°C after 3 h of solidification to determine the type of polymorph formed during isothermal crystallization. A Nicolet I_2v Polycrystalline XRD (Nicolet Instrument Corp., Madison, WI), using Cu Kα radiation with a wavelength of 0.514 nm, was used to perform powder XRD measurements. Data analysis was performed using a Siemens Polycrystalline Software Package (Micro-VAX release 2.41, June 1989; Madison, WI). The diffraction patterns were measured between angles of 5 and 32° (2θ), with a counting time of 2 s and step width of 0.05°.

RESULTS AND DISCUSSION

Isothermal crystallization kinetics were characterized in terms of induction time and the empirical Avrami equation for crystallization of pure fats (ICCB, AMF, and AMF fractions) as well as blends of ICCB with AMF or its fractions at 15°C.

Component fats. The plots of the fraction of crystals vs. time for component fats are given in Figure 2. ICCB crystallized after 10 min, and crystallization was completed in about 35 min. AMF and its fractions crystallized faster than ICCB. The SS and 32S fractions completed almost half of the crystallization in the first 5 min. Crystallization of high-melting fractions was slower than for very high-melting fractions. The low-melting fractions (17S and 17L) did not crystallize during 3 h at 15°C. ICCB, AMF, and AMF fractions, except for 17S and 17L, crystallized in β′-form as verified from both their X-ray diffraction patterns and melting peak temperatures, obtained from DSC melting curves following isothermal crystallization.

The shape of crystal fraction vs. time can give important clues for the crystallization mechanism of a particular substance (36). Noticeable differences in the shape of the curves of the component fats can be observed (Fig. 2). This may suggest different crystallization mechanisms for the component fats. The shape of the ICCB curve was significantly different than that of the milk fat components. AMF also had a different curve shape compared to the milk fat fractions, although the 28S fraction exhibited a similar curve to AMF. Very high-melting fractions had similar-shaped curves, with the SS and 32S fractions being more similar to each other than to the 30S fraction. However, more precise analysis requires determina-

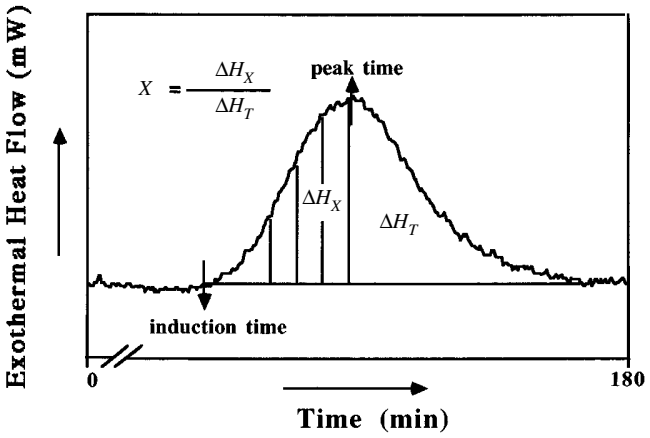

FIG. 1. Calculation of crystal fraction (X) as a function of time for the isothermal crystallization curve at 15°C, obtained by differential scanning calorimeter for the blend of 5% solid milk fat fraction obtained at 27°C then 32°C super stearin (SS) with 95% Ivory Coast cocoa butter (ICCB). ΔH_X and ΔH_T represent partial enthalpy and total enthalpy of crystallization, respectively. mW = milli-Watts.

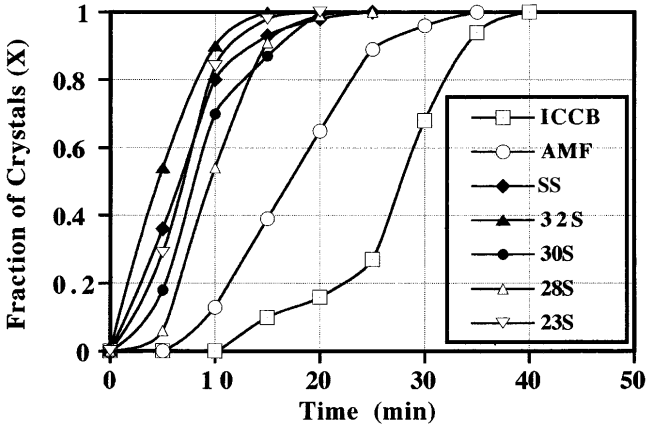

FIG. 2. Fraction of crystals as a function of time for isothermal crystallization at 15°C for ICCB, anhydrous milk fat (AMF), and AMF fractions: solid at 27°C then 32°C (SS), 32°C (32S), 30°C (30S), 28°C (28S), and 23°C (23S). For other abbreviations see Figure 1.

tion of *n*, since it has been stated that the difference between two plots, one with $n = 4$ and the other with $n = 3$, may not be very great (36). Additionally, Figure 2 clearly points out that AMF and the milk fat fractions crystallized very rapidly compared to ICCB.

The Avrami plots for component fats are given in Figure 3. The data generally showed a very good fit to the Avrami equation ($R = 0.993–0.998$). The *n* and *k* values were calculated from the slope and y-intercept of the plots, respectively. The results obtained from Avrami analysis of the DSC isothermal data are given in Table 2 for component fats. For ICCB, the *n* was 4.1, whereas for AMF and its fractions, the *n* was between 1.9 and 3.3. Statistical analysis using Fisher's least significant difference (analysis of variance-one way) test at the 95% confidence interval (CI) was performed on the *n* of the component fats (Table 2). Statistically significant differences between ICCB, AMF, and milk fat fractions were found. No significant difference was found among the very high-melting milk fat fractions or among the high-melting milk fat fractions, or between AMF and the high-melting fractions. However, the *n* of very high-melting fractions and AMF were significantly different (CI = 95%). An *n* of 4 might indicate heterogeneous nucleation and crystal development in spheres from sporadic nuclei (32). It also suggests that nucleation rate is a constant and independent of time (33). Values of *n* of 4 were reported by Kawamura (28) for palm oil and by Ziegleder (29) for cocoa butter, which were similar to the *n* for ICCB found in this study. The *n* of 3 for AMF also suggests spherulitic growth, but from instantaneous nuclei. This corresponds to the case where the great majority of the nuclei form near the beginning of crystallization (32), and nucleation rate decreases with time (33). For very high-melting milk fat fractions, the *n* of 2 might indicate plate-like growth, where growth is primarily along two dimensions. The *n* of 2 also suggests that nucleation rate is very rapid at the beginning, but decreases with time (33). These results suggest that differences in chemical composition of fats might lead to different crystallization mechanisms.

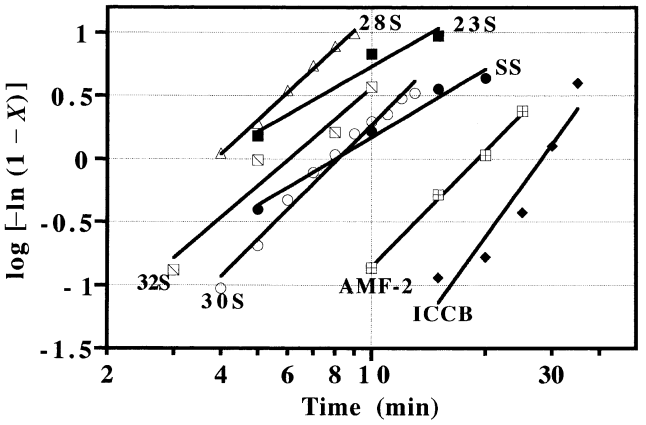

FIG. 3. Avrami plots for ICCB, AMF, and AMF fractions: solid at 27°C then 32°C (SS), 32°C (32S), 30°C (30S), 28°C (28S), and 23°C (23S). For abbreviations see Figures 1 and 2.

Capillary m.p. measures the melting temperature of high-melting glycerides. The m.p. of the milk fat fractions decreased as the fractionation temperature decreased (Table 1). Since the m.p. of the fats are different, the degree of supercooling should be different for each sample when they crystallized at 15°C. Figure 4 shows the plot of *n* vs. capillary melting temperature for the component fats. A high degree of correlation was found between the m.p. of the fractions and the *n*. The SS fraction had the lowest *n* and had the highest melting temperature. In general, as the m.p. decreased, the value of the *n* increased, except for the 28S fraction. In other words, as the degree of supercooling decreased, *n* values increased. This may be related to suggested crystallization mechanisms. Spherulitic growth starts initially from small rod-like, plate-like, or needle-like crystals (36,37). If nucleation density is extremely high, spherulitic development may not be attained (36). The very high-melting fractions may

TABLE 2
Avrami Exponent (*n*), Crystallization Rate Constant (*k*), and Half-Time for Crystallization ($t_{1/2}$) Calculated by Avrami Plots of the Isothermal Crystallization Curves at 15°C Obtained from Differential Scanning Calorimeter for Ivory Coast Cocoa Butter (ICCB), Anhydrous Milk Fat (AMF), and AMF Fractions[a]

Fat Type	*n*	$k \times 10^{-4}$ (min)	$t_{1/2}$ (min)
ICCB	4.1 ± 0.1 (A)[b]	0.020 ± 0.010 (A)	23.2 ± 2.1 (A)
AMF	3.0 ± 0.2 (B,C)	1.630 ± 0.500 (A)	17.3 ± 1.6 (B)
SS	1.6 ± 0.3 (D)	407.5 ± 236.0 (B)	6.20 ± 0.4 (D,E)
32S	1.9 ± 0.6 (D)	389.0 ± 310.0 (B)	5.20 ± 1.2 (E)
30S	2.1 ± 0.7 (C,D)	108.0 ± 83.00 (A,B)	8.80 ± 1.4 (C,D)
28S	3.3 ± 0.0 (A,B)	3.300 ± 0.800 (A)	10.3 ± 0.8 (C)
23S	2.4 ± 0.4 (B,C,D)	107.8 ± 104.8 (A,B)	6.80 ± 0.80 (D,E)

[a]Solid at 27°C then 32°C (SS), 32°C (32S), 30°C (30S), 28°C (28S), and 23°C (23S).
[b]Mean values of three replicates with standard deviation. Different letters (A,B,C,D,E) denote significantly different groups ($P < 0.05$), whereas same letters denote similar groups in each column ($P > 0.05$).

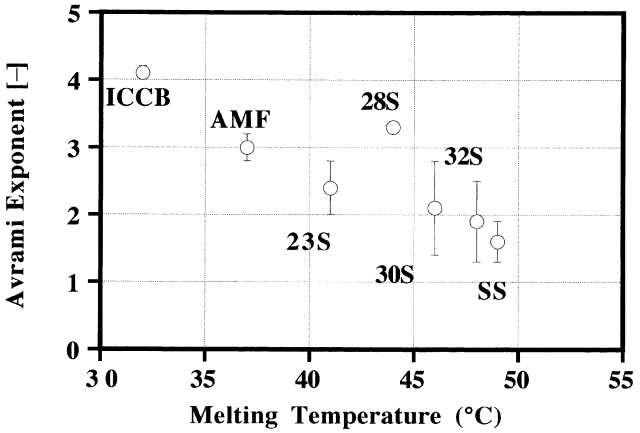

FIG. 4. Avrami exponents vs. melting temperatures of component fats. ICCB, AMF, and AMF fractions: solid at 27°C then 32°C (SS), 32°C (32S), 30°C (30S), 28°C (28S), and 23°C (23S). For abbreviations see Figures 1 and 2.

have higher nucleation density at 15°C compared to ICCB, AMF, and high-melting fractions, due to the higher degree of supercooling. This may enhance the possibility of existence of only plate-like crystals in the very high-melting fractions. A plate-like crystal can probably convert into a spherulite only if nucleation density decreases in a system. Therefore, differences in crystallization mechanism and geometry of crystals may be related to the differences in chemical composition.

It was reported (37) that in suspension crystallization with agitation, spherulite milk fat crystals were formed by the growth of small needle crystals at 30°C. However, at 20°C, after removal of 30°C solid fraction, aggregates formed from smaller and thinner needle crystals. Since only static crystallization (i.e., no agitation) can be studied by DSC, needle-like crystals may not aggregate into spherulites when the nucleation density is high, as in the very high-melting milk fat fractions. Polymorphism also may be an important parameter influencing the suggested crystallization mechanisms for the component fats. As mentioned previously, XRD analysis of pure fats showed that all crystallized in β′-form at 17°C. However, glycerides may crystallize in different shapes for the same polymorphic form (38), although kinetics of polymorphic transformations have not been studied.

Induction time is defined as the point where a fraction of crystals can be detected experimentally to be different from zero (36). It has been shown that for polymers for a given average rate of crystallization, as induction time increases, the *n* gets higher in value (36). In order to check the validity of this statement in our system, Avrami exponents of pure fats were plotted vs. induction time determined from the crystallization curves. As reported in a previous work (17), milk fat and milk fat fractions had shorter induction times for nucleation and peak time (approximated as rate of crystallization) than cocoa butter during isothermal crystallization at 15°C. Table 3 shows induction time for nucleation for component fats and blends of ICCB with AMF or its fractions, taken from our previous work (17). Figure 5 shows *n* as a function of induction time for pure fats. As the induction time of pure fats increased, the *n* generally was higher. Again, *n* of the 28S fraction was higher than expected based on this relationship.

The *k* values are shown in Table 2. As mentioned previously, *k* is a function of nucleation and growth rates (36). It can be used to provide a quantitative description of crystallization if nucleation and growth rate can be determined separately by other measurement techniques, such as microscopy or synchrotron XRD. No significant difference was found in *k* values between ICCB and AMF, 30S, and high-melting fractions. However, the SS and 32S fractions had significantly higher *k* values (CI = 95%). No significant difference was found either among the very high-melting fractions or between SS, 32S, 30S, and 23S fraction (CI = 95%). In general, as the *n* values decreased, *k* values increased, although the high degree of uncertainty in this data makes this relationship difficult to observe. The high value of *k* for the very high-melting fractions may indicate the high rate of nucleation in these fat fractions.

The $t_{1/2}$ was calculated as 23.2 min for ICCB and 17.3 min for AMF (Table 2). The half-time for crystallization of ICCB was statistically different than those for AMF and its fractions (CI = 95%). Figure 2 clearly illustrates that ICCB crystallized more slowly than AMF-2 and its fractions. In general, as m.p.

TABLE 3
Induction Time for Nucleation for Component Fats and Blends of ICCB with AMF or AMF Fractions[a]

Fat type	% in mixture	Induction time (min)
ICCB	100	9.4 ± 1.2[b]
AMF	5	13.2 ± 0.8
	10	15.3 ± 0.9
	100	2.6 ± 0.4
SS	5	12.7 ± 3.0
	10	20.8 ± 3.5
	100	1.4 ± 0.2
32S	5	11.9 ± 0.8
	10	10.1 ± 6.1
	100	0.8 ± 0.4
30S	5	15.2 ± 0.7
	10	20.8 ± 1.0
	100	1.8 ± 0.4
28S	5	12.3 ± 2.7
	10	16.0 ± 1.3
	100	1.8 ± 0.6
23S	5	21.9 ± 10.6
	10	46.2 ± 2.3
	100	2.2 ± 0.2
17S	5	17.9 ± 1.2
	10	29.0 ± 2.9
	100	N[b]
17L	5	11.9 ± 1.5
	10	20.6 ± 1.4
	100	N

[a]Solid at 27°C then 32°C (SS), 32°C (32S), 30°C (30S), 28°C (28S), 23°C (23S), 17°C (17S), and Liquid at 17°C (17L).
[b]Mean value of three replicates with standard deviation.
[b]N = no crystallization was observed in 3 h. See Table 2 for abbreviations.

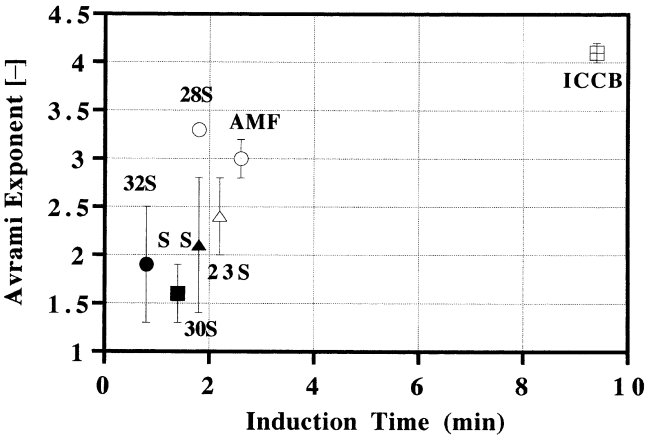

FIG. 5. Avrami exponent vs. induction time for component fats. ICCB, AMF, and AMF fractions: solid at 27°C then 32°C (SS), 32°C (32S) and 30°C (30S), 28°C (28S), and 23°C (23S). For abbreviations see Figures 1 and 2.

of fractions decreased, the $t_{1/2}$ increased, except for the 23S fraction. The chemical structure of this fraction was similar to the very-high melting fractions, which has been reported previously (17). The 23S fraction was enriched in longer-chain saturated fatty acids, and had slightly lower concentration of short-chain fatty acids, compared to the other high-melting fraction, 28S. All milk fat fractions had shorter half-time for crystallization (statistically significant at CI = 95%) than AMF. The 32S fraction had the shortest $t_{1/2}$ among the milk fat fractions, although statistical analysis showed no significant differences among very high-melting fractions.

Binary fat blends. The binary fat blends of ICCB with AMF crystallized more slowly than pure ICCB, with 10% addition having more retardation effect than 5% addition. The addition of milk fat fractions showed similar effects as AMF on the amount of ICCB crystallized, except for the 32S fraction. This fraction enhanced crystallization in the binary fat blends, with 10% addition having more effect than 5%. This might be due to the specific interactions of the acylglycerols of the two fats. Ten percent addition of 23S delayed the crystallization of ICCB to the greatest extent compared to the other additives. It also should be noted here that all binary blends of ICCB with AMF or its fractions crystallized in β′-form; this was verified from both their XRD patterns and DSC melting curves following isothermal crystallization.

The data generally showed a very good fit to the Avrami equation, although the data for cocoa butter exhibited some curvature. The *n* varied between 4.1 and 7.1 among the binary fat blends, with the blend of 10% 17S with ICCB having the highest *n* (Table 4). The *n* of 4 or above for the binary blends suggest heterogeneous nucleation and spherulite crystal development from sporadic nuclei (32). These values suggest that addition of 5 and 10% AMF and its fractions to ICCB did not change the mechanism for nucleation and growth of ICCB (27,32). However, it has been suggested that *n* larger than 4 indicate that nucleation rate increases with time (27,33), although this contention was not verified in our data. Statistical analysis of *n* of the fat blends showed significant differences (CI = 95%) (Table 4). At 5% additive level, 30S, 23S, 17S, and 17L fractions significantly changed the *n* of ICCB, whereas the others did not (CI = 95%). Higher and statistically different Avrami values for the blends of ICCB with 5% 30S, 23S, 17S, and 17L fractions may be the result of a decrease in the *k* in these blends. Thus, the low *k* values may indicate a decrease in nucleation and/or growth rate in these fat blends since *k* is a combined function of nucleation and growth (Table 4). Pure ICCB had the highest *k* value among the fats, but the difference with the 5% blends was not statistically significant (CI = 95%).

Addition of 5% AMF and its fractions did not change the melting peak temperature of ICCB (CI = 95%). Consequently, it can be concluded that 5% addition of AMF and its fractions to ICCB generally resulted in the occurrence of higher Avrami values in the blends, but the overall crystallization mechanism of ICCB did not change. At 5% additive level, $t_{1/2}$ of ICCB was greatly increased by the addition of AMF and its fractions, with the 23S fraction having the largest half-time. However, statistical analysis did not show significant differences in $t_{1/2}$ between ICCB and its blends, except for the 23S fraction (CI = 95%).

TABLE 4
The *n*, *k*, and $t_{1/2}$ Calculated by Avrami Plots of the Isothermal Crystallization Curves at 15°C Obtained from Differential Scanning Calorimeter for Blends of ICCB with 5 and 10% AMF or AMF Fractions[a]

Fat type	*n*	$k \times 10^{-4}$ (min)	$t_{1/2}$ (min)
ICCB	$4.1 \pm 0.1^{(G,H)b}$	$2000 \pm 1000^{(A)}$	$23.2 \pm 2.1^{(A)}$
5% AMF-2	$4.3 \pm 0.0^{(G,H,F)}$	$263 \pm 9^{(B)}$	$31.2 \pm 10.2^{(D,E,F)}$
10% AMF-2	$4.2 \pm 0.5^{(G,H)}$	$308 \pm 421^{(B)}$	$40.8 \pm 10.2^{(B,C,D)}$
5% SS	$4.5 \pm 0.4^{(E,F,G,H)}$	$193 \pm 190^{(B)}$	$32.2 \pm 0.3^{(D,E,F)}$
10% SS	$5.3 \pm 1.2^{(C,D,E)}$	$23 \pm 33^{(B)}$	$45.3 \pm 8.6^{(B)}$
5% 32S	$4.8 \pm 0.1^{(E,F,G,H)}$	$176 \pm 97^{(B)}$	$24.1 \pm 0.7^{(G,F)}$
10% 32S	$4.9 \pm 1.4^{(E,F,G,H)}$	$5250 \pm 740^{(B)}$	$20.4 \pm 4.4^{(G)}$
5% 30S	$5.3 \pm 0.1^{(C,D,E)}$	$6 \pm 1^{(B)}$	$32.4 \pm 0.6^{(D,E,F)}$
10% 30S	$5.0 \pm 0.3^{(D,E,F,G)}$	$4 \pm 3^{(B)}$	$46.7 \pm 4.0^{(B)}$
5% 28S	$4.5 \pm 0.5^{(E,F,G,H)}$	$364 \pm 523^{(B)}$	$30.5 \pm 2.9^{(E,F)}$
10% 28S	$4.0 \pm 0.2^{(H)}$	$364 \pm 356^{(B)}$	$40.1 \pm 1.3^{(B,C,D,E)}$
5% 23S	$5.9 \pm 0.3^{(B,C,D)}$	$6 \pm 8^{(B)}$	$42.6 \pm 21.8^{(B,C)}$
10% 23S	$6.5 \pm 0.3^{(A,B)}$	$0.001 \pm 0.001^{(B)}$	$77.2 \pm 5.0^{(A)}$
5% 17S	$6.2 \pm 0.2^{(A,B,C)}$	$0.4 \pm 0.2^{(B)}$	$32.9 \pm 2.7^{(C,D,E,F)}$
10% 17S	$7.1 \pm 1.0^{(A)}$	$0.01 \pm 0.01^{(B)}$	$49.6 \pm 1.3^{(B)}$
5% 17L	$5.2 \pm 0.3^{(D,E,F)}$	$4.8 \pm 3.9^{(B)}$	$26.6 \pm 4.2^{(G,F)}$
10% 17L	$4.4 \pm 0.3^{(E,F,G,H)}$	$2.4 \pm 1.4^{(B)}$	$49.7 \pm 4.6^{(B)}$

[a]Solid at 27°C then 32°C (SS), 32°C (32S), 30°C (30S), 28°C (28S), and 23°C (23S), 17°C (17S), and liquid 17°C (17L).
[b]Mean values of three replicates with standard deviation. Different superscript letters (A–H) denote significantly different groups ($P < 0.05$), whereas same letters denote similar groups in each column. See Table 2 for abbreviations.

At 10% additive level (Table 4), only addition of the SS, 23S, and 17S fractions to ICCB caused a significant increase in *n* (CI = 95%). The *k* of the fat blends and pure ICCB were statistically similar (CI = 95%), except for the blend of ICCB with 32S, which had statistically different *k* value than the other blends (CI = 95%). In general, the blends with higher *n* had lower *k* values. Moreover, the low *k* values may indicate a decrease in either nucleation or growth rate in these fat blends (Table 4) since *k* is a function of both. Although *n* did not suggest any change in the crystallization mechanism of ICCB by the addition of AMF and its fractions, the additives generally caused more pronounced retardation in the $t_{1/2}$ of ICCB, except for the 32S fraction (CI = 95%). However, the difference between pure ICCB and its blend with 32S was not statistically different (CI = 95%). The 23S fraction caused the greatest increase in $t_{1/2}$ of ICCB, and the low-melting fractions followed the 23S fraction. There was no significant difference in $t_{1/2}$ of ICCB between the 17S and 17L fractions.

As reported previously (17), induction time for nucleation of cocoa butter was increased by the additives depending on the type and addition level (Table 3). Milk fat and low-melting milk fat fractions retarded the nucleation of cocoa butter to a greater extent than very high- and high-melting milk fat fractions, with 10% addition having more effect than 5% addition. Figures 6 and 7 show *n* as a function of induction time for binary fat blends of ICCB with 5 and 10% additives, re-

spectively. As discussed previously, binary fat blends of ICCB with 5 and 10% additives had higher *n* values than pure ICCB. Induction time of ICCB was increased by the additives, with 10% addition having more effect. Figures 6 and 7 also show that as induction time increased (i.e., nucleation rate decreased), *n* values increased. As mentioned previously, it has been suggested that Avrami values higher than 4 indicate an increase in nucleation rate with time (27,33); however, this contention was not verified in our study.

The $t_{1/2}$ is a combined function of *k* and *n* (36). Since $t_{1/2}$ is derived from the Avrami equation, it shows the time when crystal fraction reaches 50% (36). Evaluation of crystal fractions of the fats (both pure and blends) as a function of time showed that 50% fraction of crystals (i.e., half of the crystallization) generally occurred halfway through crystallization, as determined from Equation 2 in both component fats and binary fat blends. Excellent correlation was found between the $t_{1/2}$ for pure fats and binary fat blends, as well as the sum of the induction time and peak time (from zero time to peak time) ($R = 0.987$, 0.912, and 0.985 for pure fats, 5%, and 10% addition of additives to ICCB, respectively) for isothermal crystallization of these fats, as shown in Tables 5 and 6. Note that crystallization peak times for component fats and binary blends at 15 °C were taken from our previous work (17). This suggests that the crystallization peak occurred when about 50% of molten fat transformed into crystals under the conditions used in this study.

Consequently, isothermal crystallization data gave a very good fit to the Avrami equation. The results may give a quantitative explanation for the slow crystallization of ICCB in the presence of milk fat or milk fat fractions by employing the Avrami equation. However, it is not possible to determine nucleation and growth behavior of a phase transformation based on the time dependence of transformed volume. It is essential to have additional knowledge about the process, best gained from direct microscopic observations of the transforming particles as a function of time.

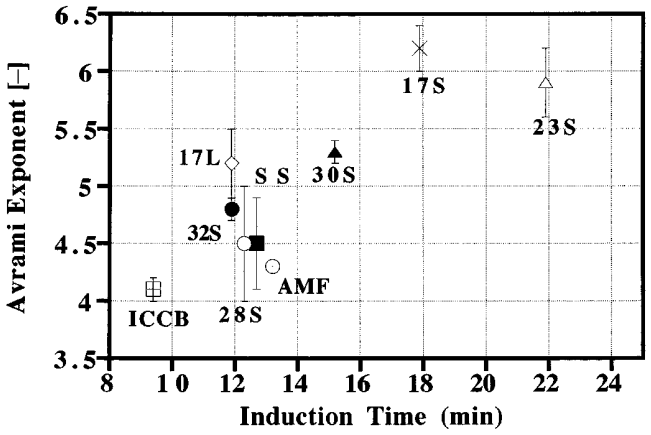

FIG. 6. Avrami exponent vs. induction time for the blends of ICCB with 5% AMF and AMF fractions: solid at 27°C then 32°C (SS), 32°C (32S) and 30°C (30S), 28°C (28S), 23°C (23S), 17°C (17S), and liquid at 17°C (17L). For abbreviations see Figures 1 and 2.

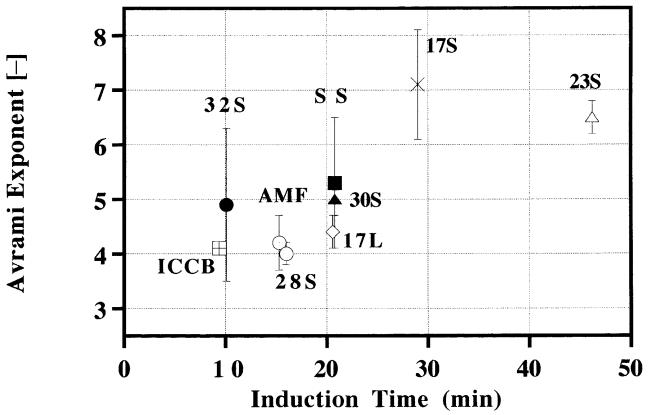

FIG. 7. Avrami exponent vs. induction time for the blends of ICCB with 10% AMF, and AMF fractions: solid at 27°C then 32°C (SS), 32°C (32S) and 30° C (30S), 28°C (28S), 23°C (23S), 17°C (17S) and liquid at 17°C (17L). For abbreviations see Figures 1 and 2.

TABLE 5
Correlation Between $t_{1/2}$ Calculated by Avrami Plots and Induction Time (t_i) Plus Peak Time (t_p) from the Isothermal Crystallization Curves at 15°C Obtained from Differential Scanning for ICCB, AMF or AMF Fractions[a]

Fat type	$t_{1/2}$ (min)	$t_i + t_p$ (min)
ICCB	23.2 ± 2.1[a]	25.8 ± 4.5
AMF-2	17.3 ± 1.6	15.8 ± 0.5
SS	6.20 ± 0.4	4.70 ± 0.00
32S	5.20 ± 1.20	4.00 ± 0.50
30S	8.80 ± 1.40	6.20 ± 0.90
28S	10.3 ± 0.8	10.6 ± 2.1
23S	6.80 ± 0.8	6.30 ± 1.20

[a]Solid at 27°C then 32°C (SS), 32°C (32S), 30°C (30S), 28°C (28S), and 23°C (23S). Data for ($t_i + t_p$) taken from Metin and Hartel (1996; Ref. 17).
[b]Mean values of three replicates with standard deviation. See Table 2 for other abbreviations.

REFERENCES

1. Chaiseri, S., and P.S. Dimick, Cocoa Butter—Its Composition and Properties, *Manuf. Confect. 67*:115–122 (1987).
2. Ziegleder, V.G., Crystallization of Chocolate Masses. Part 1, *Zucker-u-Suss. Wirt. 41*:165–168 (1988).
3. Hartel, R.W., Applications of Milk-Fat Fractions in Confectionery Products, *J. Am. Oil Chem. Soc. 73*:944–953 (1996).
4. Metin, S., J. Fabian, and R.W. Hartel, Milk Fat Crystallization: An Overview, in *Proceeding of Bremer International Workshop on Industrial Crystallization*, University of Bremen, Bremen, Germany, 1996, pp. 61–69.
5. Chapman, G.M., E.E. Akehurst, and W.B. Wright, Cocoa Butter and Confectionery Fats. Studies Using Programmed Temperature X-Ray Diffraction and Differential Scanning Calorimetry, *J. Am. Oil Chem. Soc. 48*:824–830 (1971).
6. Jewell, G.G., and L. Bradford, Considerations in Chocolate Formulation, *Manuf. Conf. 61*:26–30 (1981).
7. Edwards, W.P., Uses for Dairy Ingredients in Confectionery, *J. Soc. Dairy Technol. 37*:122–125 (1984).
8. Kaylegian, K.E., and R.C. Lindsay, *Handbook of Milk Fat Fractionation Technology and Application*, AOCS Press, Champaign, 1995.
9. Timms, R.E., The Phase Behaviour of Mixtures of Cocoa Butter and Milk Fat, *Lebensm. Wiss. Technol. 13*:61–65 (1980).

TABLE 6
Correlation Between $t_{1/2}$ Calculated by Avrami Plots and t_i Plus t_p from the Isothermal Crystallization Curves at 15°C Obtained from Differential Scanning Calorimetry for Blends of ICCB with 5 and 10% AMF or AMF Fractions[a]

Fat type	$t_{1/2}$ (min)	$t_i + t_p$ (min)
ICCB	23.2 ± 2.1[b]	25.8 ± 4.5
5 % AMF-2	31.2 ± 0.2	34.7 ± 0.4
10% AMF-2	40.8 ± 3.5	43.8 ± 0.8
5% SS	32 ± 0.3	31.9 ± 1.8
10% SS	45.3 ± 8.6	50.3 ± 8.4
5% 32S	24.1 ± 0.7	22.5 ± 0.3
10% 32S	20.4 ± 4.4	20.5 ± 4.7
5% 30S	32.4 ± 0.6	35.5 ± 2.1
10% 30S	46.7 ± 4.0	49.8 ± 2.0
5% 28S	30.5 ± 2.9	33.9 ± 2.9
10% 28S	40.1 ± 1.3	46.7 ± 1.3
5% 23S	42.6 ± 21.8	40.2 ± 19.8
10% 23S	77.2 ± 5.0	74.5 ± 5.2
5% 17S	32.9 ± 2.7	32.1 ± 2.5
10% 17S	49.6 ± 1.3	48.4 ± 2.4
5% 17L	26.6 ± 4.2	29.4 ± 5.6
10% 17L	49.7 ± 4.6	52.2 ± 2.9

[a]Solid at 27°C then 32°C (SS), 32°C (32S), 30°C (30S), 28°C (28S), and 23°C (23S). Data for ($t_i + t_p$) taken from Metin and Hartel (1996; Ref. 17).
[b]Mean values of three replicates with standard deviation. See Tables 2 and 5 for abbreviations.

10. Campbell, L.B., A. Anderson, and P.G. Keeney, Hydrogenated Milk Fat as an Inhibitor of the Fat Bloom Defect in Dark Chocolate, *J. Dairy Sci. 52*:976–979 (1969).
11. Hendrickx, H., H. DeMoor, A. Huyghebaert, and G. Janssen, Manufacture of Chocolate Containing Hydrogenated Butterfat, *Rev. Int. Choc. 26*:190–193 (1971).
12. Timms, R.E., and J.V. Parekh, The Possibilities for Using Hydrogenated, Fractionated or Interesterified Milk Fat in Chocolate, *Lebensm. Wiss. Technol. 13*:177–181 (1980).
13. Barna, C.M., R.W. Hartel, and S. Metin, Incorporation of Milk Fat Fractions into Milk Chocolates, *Manuf. Conf. 72*:107–116 (1992).
14. Bystrom, C.E., and R.W. Hartel, Evaluation of Milk Fat Fractionation and Modification Techniques for Creating Cocoa Butter Replacers, *Lebensm. Wiss. Technol. 27*:142–150 (1994).
15. Lohman, M.H., and R.W. Hartel, Effect of Milk Fat Fractions on Fat Bloom in Dark Chocolate, *J. Am. Oil Chem. Soc. 71*:267–276 (1994).
16. Wood, J.S., Milk-Fat Fraction Incorporation in Dark and Milk Chocolate, Master's Thesis, University of Wisconsin, Madison, 1994.
17. Metin, S., and R.W. Hartel, Crystallization Behavior of Blends of Cocoa Butter and Milk Fat or Milk-Fat Fractions, *J. Thermal Anal. 47*:1527–1544 (1996).
18. Metin, S., Crystallization Behavior and Kinetics of Blends of Cocoa Butter and Milk Fat or Milk Fat Fractions, Ph.D. Thesis, University of Wisconsin, Madison, 1997.
19. Kissinger, H.E., Reaction Kinetics in Differential Thermal Analysis, *Anal. Chem. 29*:1702–1706 (1957).
20. Ozawa, T., Kinetics of Non-Isothermal Crystallization, *Polymer 12*:150–158 (1971).
21. Duswalt, A.A., The Practice of Obtaining Kinetic Data by Differential Scanning Calorimetry, *Thermochim. Acta 8*:57–68 (1974).
22. Augis, J.A., and J.E. Bennett, Calculation of the Avrami Parameters for Heterogeneous Solid State Reactions Using a Modification of the Kissinger Method, *J. Thermal Anal. 13*:283–292 (1978).
23. Henderson, D.W., Thermal Analysis of Non-Isothermal Crystallization Kinetics in Glass Forming Liquids, *J. Non-Crystalline Solids 30*:301–315 (1979).
24. Weinberg, M.C., On the Analysis of Non-Isothermal Thermoanalytic Crystallization Experiments, *J. Non-Crystalline Solids 127*:151–158 (1991).
25. Woldt, E., The Relationship Between Isothermal and Nonisothermal Description of Johnson-Mehl-Avrami-Komogorov Kinetics, *J. Phys. Chem. Solids 53*:521–527 (1992).
26. Graydon, J.W., S.J. Thorpe, and D.W. Kirk, Determination of the Avrami Exponent for Solid State Transformations from Non-Isothermal Differential Scanning Calorimetry, *J. Non-Crystalline Solids 175*:31–43 (1994).
27. Christian, J.W., *The Theory of Transformations in Metals and Alloys*, 2nd edn., Pergamon Press, London, 1975.
28. Kawamura, K., The DSC Thermal Analysis of Crystallization Behavior in Palm Oil, *J. Am. Oil Chem. Soc. 56*:753–758 (1979).
29. Ziegleder, V.G., DSC—Thermal Analysis and Kinetics of Cocoa Butter Crystallization, *Fat Sci. Technol. 92*:481–485 (1990).
30. Herrera, M.L., and F.J. Marques Rocha, Effects of Sucrose Esters on the Kinetics of Polymorphic Transition in Hydrogenated Sunflower Oil, *J. Am. Oil Chem. Soc. 73*:321–326 (1996).
31. Dibildox-Alvarado, E., and J.F. Toro-Vazques, Isothermal Crystallization of Tripalmitin in Sesame Oil, *Ibid. 74*:69–76 (1997).
32. Avrami, M., Kinetics of Phase Change. II. Transformation–Time Relations for Random Distribution of Nuclei, *J. Chem. Phys. 8*:212–224 (1940).
33. Doremus, R.H., *Rates of Phase Transformations*, Academic Press, Orlando, 1985, pp. 24–26.
34. Arvanitoyannis, I., and J.M.V. Blanshard, Rates of Crystallization of Dried Lactose–Sucrose Mixtures, *J. Food Sci. 59*:197–205 (1994).
35. *Official Methods and Recommended Practices of the American Oil Chemists' Society,* 3rd edn., AOCS, Champaign, 1973, Method Cc 1-25.
36. Sharples, A., *Introduction to Polymer Crystallization*, Edward Arnold Publishers, Ltd., London, 1966, pp. 4–60.
37. Ahza, A.B., *Kinetics of Milk Fat Crystallization in a Continuous Crystallizer*, Ph.D. Thesis, University of Wisconsin, Madison, 1995.
38. Chapman, D., The Polymorphism of Glycerides, *Chem. Rev. 62*:433–456 (1962).

[Received December 1, 1997; accepted July 16, 1998]